

28 **ORIGINALITY-SIGNIFICANCE STATEMENT**

29 This study reveals that sulfide oxidation within an anoxic layer of purple sulfur bacteria in the stratified
30 water column of Lake Cadagno is largely coupled to oxygen consumption. Our findings imply that aerobic
31 metabolism may be more prevalent in anoxic zones than previously thought. We also present a
32 metagenome-assembled genome of *Chromatium okenii* which is the first genome sequence for the genus
33 *Chromatium* and reveals new interesting physiological features of this environmentally relevant organism
34 including its capacity for aerobic respiration.

35 **SUMMARY**

36 Anoxygenic phototrophic sulfide oxidation by purple and green sulfur bacteria plays a key role in
37 sulfide removal from anoxic shallow sediments and stratified waters. Although some purple sulfur
38 bacteria can also oxidize sulfide with nitrate and oxygen, little is known about the prevalence of
39 this chemolithotrophic lifestyle in the environment. In this study, we investigated the role of
40 *Chromatium okenii* in chemolithotrophic sulfide removal in the chemocline of Lake Cadagno. This
41 purple sulfur bacterium appears to remain active during the night, as evidenced by its continued
42 motility and O₂-driven carbon fixation. Our temporally resolved, high-resolution chemical profiles
43 revealed that sulfide oxidation is largely driven by aerobic respiration in the anoxic chemocline.
44 We postulate that the abundant and highly active *Chr. okenii* are, at least in part, responsible for
45 this aerobic sulfide oxidation and that they bridge the spatially separated gradients of oxygen and
46 sulfide using a novel mechanism of transport driven by the strong convection within the
47 chemocline. The genome of *Chr. okenii* reconstructed from the Lake Cadagno metagenome
48 confirms its capacity for microaerophilic growth and provides further insights into its metabolic
49 capabilities. Altogether, our observations suggest that aerobic respiration may not only play an

50 underappreciated role in anoxic environments, but also that organisms typically considered strict
51 anaerobes may be involved.

52 INTRODUCTION

53 Anoxygenic phototrophic bacteria oxidizing sulfide and fixing CO₂ with sunlight play an important
54 role in the carbon and sulfur cycles of sulfidic, shallow sediments and stratified water columns.
55 Phototrophic sulfur bacteria, for example, are responsible for 20-85% of the total daily carbon
56 fixation in anoxic lakes (summarized in Cohen *et al.*, 1977). This primary production is so
57 important that it can control the bulk C-isotope fractionation in the water column, generating
58 isotopic signatures that are transported and preserved in sediments (Posth *et al.*, 2017). Biomass
59 from anoxygenic phototrophs feeds both grazing zooplankton in overlying oxic waters (Sorokin
60 1966) and drives sulfate reduction in anoxic waters below (Pfennig 1975). The phototrophic sulfur
61 bacteria also remove toxic sulfide from the water column enabling aerobic life at the surface while
62 recycling sulfur compounds for sulfate reducers. While their role in sulfide detoxification has long
63 been recognized in stratified lakes, there is mounting evidence that phototrophic sulfur bacteria
64 also significantly impact sulfur cycling in marine environments such as the Black Sea (Jørgensen
65 *et al.*, 1991) and the Chesapeake Bay (Findlay *et al.*, 2015).

66 Anoxygenic phototrophs generally inhabit illuminated, anoxic, reducing environments due to the
67 toxicity of oxygen to these bacteria, and to the competition with abiotic reactions involving oxygen
68 for their electron donors. Nonetheless, some anoxygenic phototrophs have evolved the capacity
69 for chemotrophic growth under microoxic conditions. Whereas the green sulfur bacteria (GSB) of
70 the *Chlorobiaceae* family are strict anaerobes, members of *Proteobacteria* collectively known as
71 the purple sulfur bacteria (PSB), can be anaerobic to microaerobic (e.g. Kampf and Pfennig, 1980;

72 de Witt and Van Gernerden, 1990). Both the GSB and PSB are well adapted to fluctuating
73 environmental conditions, synthesizing and accumulating storage compounds during periods of
74 nutrient excess. The anoxygenic phototrophs are known to store zero-valent sulfur (S^0),
75 polyphosphate, glycogen, and in the case of the PSB alone, poly-3-hydroxyalkanoates (PHA) (Mas
76 and Van Gernerden, 1995). The macromolecular structure and metabolism of these compounds
77 have been intensely studied in laboratory pure cultures in order to understand conditions leading
78 to their accumulation and breakdown. It has been suggested that glycogen may play a role in
79 energy generation under dark conditions based on observations that cultured *Chromatium* sp.
80 utilize glycogen to reduce stored sulfur, yielding sulfide and PHA (Van Gernerden, 1968).

81 Here we investigated the role of anoxygenic phototrophic bacteria in dark sulfur cycling processes
82 in Lake Cadagno, a permanently stratified lake with high sulfate concentrations of up to 1-2 mM
83 in the monolimnion. Microbial reduction of sulfate in the anoxic bottom waters and sediments
84 produces large amounts of sulfide which support dense populations of GSB and PSB in the photic
85 zone. These bacteria heavily influence the chemistry of the lake, forming a sulfide- and oxygen-
86 free chemocline of 1-2 meters in thickness. The PSB *Chromatium okenii* is by far the most active
87 of these bacteria, having been shown to play a disproportionately large role in inorganic carbon
88 and ammonium assimilation despite their low abundances (<1% of total cell numbers) in the
89 chemocline (Musat *et al.*, 2008; Posth *et al.*, 2017). In addition to their important contribution to
90 light-driven sulfide oxidation, previous studies have shown that the anoxygenic phototrophic
91 bacteria of Lake Cadagno remain active in the dark (Musat *et al.*, 2008; Halm *et al.*, 2009; Storelli
92 *et al.*, 2013). However, their mechanism of energy generation in the absence of light is not yet
93 clear. There is also evidence for dark sulfide consumption, but the electron acceptors utilized

94 remain unknown. We therefore combined high-resolution biogeochemical profiling with
95 metagenomic analyses to gain an overview of possible light-independent metabolic processes
96 impacting the sulfur biogeochemistry of Lake Cadagno. In addition to providing insights into the
97 metabolism of anoxygenic phototrophic bacteria *in situ*, we present a model to explain the
98 mechanism of dark sulfide oxidation in the chemocline of this meromictic lake.

99 **RESULTS & DISCUSSION**

100 ***Biogeochemistry of Lake Cadagno***

101 Lake Cadagno is characterized by an oxic mixolimnion and a sulfidic monolimnion spatially
102 separated from each other by a chemocline (defined by bold contour lines in Fig. 1a) free of
103 detectable oxygen (detection limit 50-100 nM) and containing very little sulfide. In August 2015,
104 oxygen disappeared just above the chemocline close to 12 m depth. The daytime increase in
105 oxygen concentrations between 11-12 m depth denotes net photosynthesis and the nighttime
106 decrease denotes net respiration (Fig. 1a). The permanent absence of oxygen in the chemocline
107 indicated that oxygen was consumed both in the day and the night.

108 Steep gradients of sulfide diffusing into the chemocline varied independently of light-dark periods
109 and the total sulfide concentration in the chemocline did not exceed 5 μ M at any time point.
110 Because the lake is meromictic, these stratified conditions were also present during other
111 sampling years (see Fig. S2 for 2013 and 2014 profiles). In 2015, the 0.5-1 m wide chemocline was
112 located around 11-12 m depth, with the exact location varying over the day most likely due to the
113 action of internal waves (Egli *et al.*, 1998). In previous years, the chemocline was up to 2 m wide
114 (Fig. S2) and remained completely sulfide-free in the dark. Conservative properties such as
115 temperature and conductivity were constant throughout the chemocline in all years sampled (Fig.

116 S1&2) indicating mixing of this zone (Sommer *et al.*, 2017). Flat conductivity profiles revealed
117 stronger mixing of the chemocline in 2013 and 2014 (Fig. S2) than in 2015 (Fig. S1) when the
118 region of constant conductivity was reduced or absent.

119 *Chr. okenii* was the most significant microorganism in the chemocline in terms of biomass,
120 accounting for ~60-80% of total microbial biovolume (Sommer *et al.* 2017), and carbon fixation
121 (Musat *et al.*, 2008). The cell abundances of *Chr. okenii* in the Lake Cadagno chemocline were
122 enumerated by flow cytometry during 2 daily cycles (Fig. 1b). Higher densities of *Chr. okenii* were
123 found in 2014 ($10^6 \cdot \text{ml}^{-1}$) than in 2015 ($10^5 \cdot \text{ml}^{-1}$). *Chr. okenii* is highly motile, swimming at speeds
124 of $\sim 27 \mu\text{m} \cdot \text{s}^{-1}$ and has been hypothesized to drive the convection and mixing of the chemocline
125 (Wüest, 1994; Sommer *et al.*, 2017). *Chromatium* are known to migrate between gradients of
126 sulfide, light, and oxygen by photo- and chemotaxis (Pfennig *et al.*, 1968). We observed that *Chr.*
127 *okenii* were positioned between oxygen and sulfide gradients, regardless of changes in depth or
128 light availability (Fig. 1a,b). Other anoxygenic phototrophs that have been consistently detected
129 in the chemocline include the PSB *Lamprocystis*, *Thiocystis* and *Thiodictyon* and several GSB of
130 the genus *Chlorobium* (Tonolla *et al.*, 1999, 2004, 2005). Together these bacteria constituted the
131 majority of the total phototrophic cells ($10^6 \cdot \text{ml}^{-1}$) in 2015, but they are considerably smaller than
132 *Chr. okenii*.

133 The oxidation of sulfide by these anoxygenic phototrophs proceeds via the formation of S^0 as an
134 obligate intermediate (Mas and Van Gemerden, 1995). This S^0 was measured as particulate sulfur
135 on $0.7 \mu\text{m}$ filters and may comprise S^0 stored intracellularly by PSB and S^0 adhering extracellularly
136 to GSB. The highest concentrations of S^0 (up to $45 \mu\text{M}$; Fig. 1c) coincided with the highest *Chr.*
137 *okenii* cell numbers (Fig. 1b) in the chemocline. It is likely that this S^0 was present in the form of

138 both elemental S and polysulfides formed by the reaction of free sulfide with intra- and
139 extracellular S⁰, as has previously been suggested in other euxinic lakes (Overmann, 1997). Our
140 analytical method for total S⁰ did not distinguish between different forms of S⁰ such as
141 cyclooctasulfur and polysulfides. However, we could confirm the presence of polysulfides inside
142 live *Chr. okenii* cells in environmental samples using Raman spectroscopy. The Raman spectrum
143 of a sulfur inclusion from *Chr. okenii* exhibited two weak peaks at 152 and 218 and a prominent
144 peak at 462 cm⁻¹ (Fig. S3) which is characteristic of linear polysulfide species (Janz *et al.*, 1976).
145 The Raman peak at ~2900 cm⁻¹ corresponds to the CH₂ and CH₃ stretching vibrations (Socrates,
146 2004), and its co-occurrence with polysulfide peaks support the theory that the sulfur chains in
147 these purple sulfur bacteria are terminated by organic end groups as reported previously (Prange
148 *et al.*, 1999).

149 Over two diurnal cycles, the S⁰ inventory (Fig. S4a), or the total amount of particulate S⁰ in the
150 chemocline, was much lower than expected from the sulfide gradients and corresponding sulfide
151 fluxes (discussed below), suggesting that stored S⁰ served only as a transient intermediate and
152 was rapidly oxidized to sulfate. No day-night trends in S⁰ accumulation were apparent in the
153 chemocline. Nevertheless, the increase in the S⁰ inventory, at several time points during the night
154 was indicative of dark sulfide oxidation.

155 In culture, *Chromatium* spp. are known to store carbon compounds like glycogen and
156 polyhydroxyalkanoates (PHAs) which have been proposed to be involved in dark sulfur
157 metabolism (Mas and van Gemerden, 1995). We therefore quantified glycogen and PHA
158 abundance in biomass samples from one day/night profile of the chemocline (Fig. 2). We could
159 not detect any PHA, but the presence of glycogen during the day and night coincided with *Chr.*

160 *okenii* cell numbers (Fig. 2). This is consistent with previous reports of glycogen storage and an
161 absence of PHA in natural populations of *Chr. okenii* (Del Don *et al.*, 1994). While the highest
162 potential cellular glycogen content ($2.38 \cdot 10^{-6}$ $\mu\text{g}/\text{cell}$) was found at the top of the chemocline
163 during the day, we observed little change in the cellular glycogen content between day and night
164 (Fig. S5). Average potential cellular glycogen decreased from $5.50 \cdot 10^{-7}$ $\mu\text{g}/\text{cell}$ during the day to
165 $5.33 \cdot 10^{-7}$ $\mu\text{g}/\text{cell}$ during the night, which represents a 3% reduction in cellular glycogen reserves.
166 This is in contrast with a previous study of storage compounds in natural populations of *Chr. okenii*
167 in Lake Cadagno which reported 50% decrease in glycogen reserves in the dark (Del Don *et al.*,
168 1994). This apparent decrease in glycogen reported previously may be a result of undersampling,
169 as our time- and depth-resolved biogeochemical profiles revealed light-dark independent
170 variations in *Chr. okenii* cell numbers and glycogen concentrations. While it has been
171 demonstrated that *Chromatium* sp. in pure cultures obtain energy from the reduction of S^0 with
172 glycogen in the dark (Van Gemerden, 1968), we could not confirm this observation for *Chr. okenii*
173 *in situ*. From our data, we conclude that storage compounds did not play a significant role in the
174 dark respiratory metabolism of *Chr. okenii* in the Lake Cadagno chemocline.

175 Sulfate was measured as the end product of sulfide oxidation, but due to the high (1-2 mM)
176 background sulfate concentrations, the comparably small concentration changes resulting from
177 sulfide oxidation processes are non-detectable. To identify regions of sulfate production in and
178 around the chemocline, we therefore determined deviations from the sulfate-conductivity mixing
179 line drawn for each profile (see Fig. S6 for details). Strong mixing of the chemocline is expected
180 to produce a linear relationship between sulfate and conductivity, and large digressions from this
181 best-fit line indicated that sulfate was produced faster than the rate of mixing. The expected

182 sulfate concentration could be extrapolated based on measured conductivity, and then
183 subtracted from the measured sulfate concentration to give excess sulfate:

$$184 \quad \text{measured } [\text{SO}_4^{2-}] - \text{expected } [\text{SO}_4^{2-}] = \text{excess } [\text{SO}_4^{2-}]$$

185 This excess sulfate was attributed to biological sulfate production. Sulfate profiles from 2015
186 plotted over two diurnal cycles exhibited a peak at the top of the chemocline in the region of
187 oxygen depletion (Fig. 1d). Interestingly, sulfate production was observed both during and at the
188 end of the night. The overlap of excess sulfate and oxygen in 2015 profiles was the first indication
189 that sulfide may be oxidized aerobically, without sunlight. Daytime sulfate production in 2014
190 related to photosynthetically active radiation (PAR) intensity (Fig. S2), suggesting that sulfide and
191 S^0 could either have been oxidized aerobically within the chemocline using *in situ*-produced
192 oxygen (Milucka *et al.*, 2015) or phototrophically. The comparatively broad biogenic sulfate peak
193 in the 2014 night profile likely reflects the broader vertical distribution of the *Chr. okenii*
194 population (Fig. S2).

195 The sulfate excess in the chemocline is not expected to be affected by sulfate reduction as no
196 sulfate reduction was detected within the chemocline in 2014 or 2015. The sulfate reduction rates
197 measured in the sulfidic zone 1 m below the chemocline were about $235 \text{ nM}\cdot\text{d}^{-1}$ and $375 \text{ nM}\cdot\text{d}^{-1}$
198 in 2014 and 2015, respectively.

199 To quantify biological sulfide consumption over time, we calculated the total sulfide flux into the
200 chemocline (Fig. S4b). Assuming that phototrophic sulfide oxidation ceases in the dark, upwards-
201 diffusing sulfide should accumulate in the chemocline at night. The expected sulfide accumulation
202 was calculated based on fluxes into the layer over a 10-h night period and compared to the actual

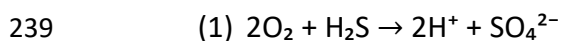
203 sulfide concentration observed in the layer. From an average sulfide flux $F = 0.15 \mu\text{m}\cdot\text{cm}^{-2}\text{h}^{-1}$ (Fig.
204 S4b), into a well-mixed layer of thickness $H = 1 \text{ m}$ over $t = 10 \text{ hours}$, the resulting sulfide
205 concentration $C = F*t/H$ should be about $15 \mu\text{M}$ in the chemocline. However, the sulfide
206 measured in the layer was about $3 \mu\text{M}$ (Fig. 1a), or five times less, indicating that sulfide is
207 consumed.

208 We therefore partitioned the total sulfide flux into two fractions: the flux of biologically consumed
209 sulfide and the flux of residual sulfide in the chemocline. First, the amount of residual sulfide was
210 calculated at each sampling time point by integrating sulfide concentrations within the mixed
211 layer (Fig. S4c). The rate of sulfide accumulation was then calculated for each 4-h sampling
212 interval and subtracted from the total sulfide flux to give the biologically consumed sulfide flux.
213 The flux of sulfide consumed in the dark was in the same range as in the day (0.03 to 0.22
214 $\mu\text{mol}\cdot\text{cm}^{-2}\text{h}^{-1}$) and the residual sulfide flux was very small in comparison (Fig. 3a). The observed
215 variations did not correlate with day-night cycles and the changes of sulfide gradients could have
216 been induced by internal waves, as mentioned above. Together, this indicates that sulfide
217 oxidation continued in the dark and seemed to be related to the total sulfide flux (Fig. S4b) rather
218 than the presence of sunlight. For comparison, the upwards flux of sulfide in previous years was
219 slightly lower, or 0.011 - $0.024 \mu\text{mol}\cdot\text{cm}^{-2}\text{h}^{-1}$ in 2013 and 0.032 - $0.072 \mu\text{mol}\cdot\text{cm}^{-2}\text{h}^{-1}$ in 2014.

220 It was not possible to calculate S^0 fluxes in Lake Cadagno because S^0 is actively transported by the
221 motile purple sulfur bacteria during chemo- and phototaxis (Pfennig *et al.*, 1968) independent of
222 diffusive processes. The total (upwards and downwards) biogenic sulfate flux (Fig. S4d) in this
223 region was roughly equivalent to the sulfide flux and followed a similar trend.

224 Overall, our high-resolution profiles revealed that sulfide in Lake Cadagno was consumed during
225 the day and night, but only light-dependent sulfide oxidation has thus far been recognized as a
226 major sulfide-removing process in the lake. In the absence of light, it is also possible that
227 alternative electron acceptors such as NO_x^- , Fe^{3+} , Mn^{4+} , or O_2 play a role in sulfide oxidation.
228 Nitrate and nitrite concentrations in the Lake Cadagno chemocline are negligible (Halm *et al.*,
229 2009; Milucka *et al.*, 2015). High fluxes of reduced, dissolved metals ($0.027 \mu\text{mol Fe}\cdot\text{cm}^{-2}\cdot\text{d}^{-1}$ and
230 $\text{Mn } 0.049 \mu\text{mol Mn}\cdot\text{cm}^{-2}\cdot\text{d}^{-1}$) suggest that Fe- and Mn-oxides are rapidly reduced by
231 microorganisms or abiotically by sulfide in the chemocline (Berg *et al.*, 2016), but re-oxidation of
232 Fe and Mn would ultimately depend on oxygen in the dark. We therefore considered oxygen as
233 the principal direct (or indirect) oxidant responsible for observed dark sulfide oxidation.

234 The oxygen flux into the chemocline varied slightly between $0.022\text{-}0.071 \mu\text{mol}\cdot\text{cm}^{-2}\cdot\text{h}^{-1}$ over the
235 period of 48 h (Fig. 3b). Oxygen fluxes measured in 2013 and 2014 were in the same range, or
236 $0.013\text{-}0.048 \mu\text{mol}\cdot\text{cm}^{-2}\cdot\text{h}^{-1}$ and $0.037\text{-}0.073 \mu\text{mol}\cdot\text{cm}^{-2}\cdot\text{h}^{-1}$, respectively. To relate oxygen fluxes to
237 sulfide consumption, we assumed a 2:1 stoichiometry between oxygen and sulfide for aerobic
238 sulfide oxidation to sulfate:



240 If all oxygen was used to respire sulfide, calculated oxygen fluxes in 2013 and 2014 were in all
241 cases sufficient to account for the sulfide oxidized in the dark. In 2015, aerobic sulfide respiration
242 could account for up to 10-50% of sulfide oxidized during the day and 5-45% of sulfide oxidized
243 during the night (Fig. 3c). During the day, the remainder of sulfide oxidation could be attributed
244 to anoxygenic photosynthesis and/or aerobic sulfide oxidation fueled by *in situ* oxygen production

245 by photosynthetic algae. At several time points in the dark, however, we could not explain the
246 disappearance of roughly 60-90% of upwards-diffusing sulfide. We hypothesize that the missing
247 oxygen is supplied laterally from the turbulent transport initiated by internal wave breaking at
248 the lake boundaries. The convection within the chemocline may be key to the transport of oxygen
249 and sulfide to aerobic sulfide-oxidizing bacteria in the chemocline. A weakening of the mixing
250 regime was observed in August 2015 (Sommer *et al.*, 2017) which may have signified a slowed
251 transport of electron acceptors, thus contributing to the accumulation of sulfide in the
252 chemocline.

253 ***Mixing and bacterial motility in Lake Cadagno***

254 To test the importance of lateral and vertical mixing, we set up simplified laboratory incubations
255 where water from Lake Cadagno chemocline was inoculated into agar-stabilized sulfide gradient
256 tubes. After five weeks of incubation under permanent light conditions, dense communities of
257 PSB developed between the gradient of upwards-diffusing sulfide and the surface colonies of
258 photosynthetic algae (Fig. S7). Microsensor profiles revealed that sulfide was completely
259 consumed at the base of the PSB layer in the light, but as soon as the light was turned off, the
260 sulfide gradient diffused upwards through the agar into the zone of purple bacteria. This is in
261 contrast to the sulfide profiles in the lake where irrespective of the day-night cycle, sulfide is
262 consistently consumed at the bottom of the chemocline. We speculate that restricted bacterial
263 motility in the agar and diffusion-limited conditions may have accounted for the differences
264 observed between our cultures and *in situ* sulfide consumption as bacterial motility and mixing
265 conditions appear necessary for continued dark sulfide oxidation in Lake Cadagno.

266 In fact, we could confirm that *Chr. okenii* are highly motile both in the day and the night by
267 performing dark field video microscopy (see Movie S1 in Supplementary Materials) of
268 environmental samples obtained during the night and monitored in a dark room to avoid any
269 light-induced artefacts. Although the average night time swimming speed of *Chr. okenii* ($9.9 \mu\text{m}$
270 s^{-1} ; see Fig. S8) was a third of the day time swimming speed ($27 \mu\text{m} \text{s}^{-1}$; Sommer et al. 2017), it is
271 clear that *Chr. okenii* remains motile even under dark conditions.

272 ***Metagenomic insights into the Chromatium okenii population in Lake Cadagno***

273 To assess whether the genomic potential supports light-independent, aerobic sulfide oxidation
274 by *Chr. okenii* in Lake Cadagno, we sequenced two metagenomes, one from the Lake Cadagno
275 chemocline and one from the phototrophic, sulfide-oxidizing enrichment culture in an agar tube
276 described above (Table S1). From a combined metagenomics assembly, we reconstructed a high
277 quality (90% complete, <1% contaminated) metagenome-assembled genome (MAG) of a PSB
278 highly abundant in the sulfur-oxidizing enrichment culture (Fig. S9). The recovered MAG had a
279 low average nucleotide identity ANI (<70%) to any sequenced *Chromatiaceae* genomes (data not
280 shown). However, it encoded an rRNA operon, including a complete 16S rRNA gene with 99%
281 sequence identity to the 16S rRNA gene of *Chr. okenii* (Imhoff et al., 1998; Tonolla et al., 1999),
282 and thus likely represents a strain of *Chr. okenii* which is the type strain of the genus *Chromatium*.
283 At this time, *Chr. okenii* has not been successfully isolated in pure culture, nor is there any
284 published genome available for this organism.

285 The key metabolic process of *Chr. okenii* in Lake Cadagno is photoautotrophic sulfur oxidation. In
286 accordance, the *Chr. okenii* MAG contained genes encoding for a sulfide : quinone reductase (*sqr*)

287 and the full genomic inventory encoding for a reverse-acting dissimilatory sulfite reductase (rDSR)
288 pathway (Fig. 4). The operon structure of the rDSR encoding genes (*dsrABEFHCMKLJOPN*) was
289 identical to the operon structure in the well described PSB model organism *Allochromatium*
290 *vinosum* (Dahl *et al.*, 2005), but no *dsrR* and *dsrS* gene were found. No genes encoding for sulfur
291 oxidation via the SOX pathway, or homologues of sulfur globule proteins (*sgpABC*) typically found
292 in PSB were detected in the draft genome. In line with its phototrophic metabolism, the *Chr.*
293 *okenii* MAG showed the genomic potential for photosynthesis, with the genes encoding for a light
294 harvesting complex 1 (*pufAB*) and a PSB-type photosynthetic reaction center (*pufLMC*) encoded
295 in a single operon. Furthermore, the full genomic repertoire for a NADP-Me type C4
296 photosynthetic carbon assimilation cycle, and all genes (with exception of *cbbS* encoding for the
297 small subunit of the ribulose-1,5-bisphosphate carboxylase/oxygenase) necessary for CO₂
298 assimilation via the Calvin-Benson-Bassham (CBB) Cycle were present (Fig. 4).

299 Many *Chromatiaceae* can grow chemoautotrophically, respiring oxygen under microoxic
300 conditions (Kämpf and Pfennig, 1980). Cytochrome (Cyt) *c*-containing oxidases (e.g. Cyt *aa3*, Cyt
301 *cbb3*) were not found in the *Chr. okenii* MAG. However, a Cyt *bd* type ubiquinol oxidase, known to
302 function as sulfide-resistant O₂-accepting oxidase in other *Gammaproteobacteria* (Forte *et al.*,
303 2016), was identified (Fig. 4). Further, a plethora of genes related to heme *b* (*gltX*, *hemALBCD*,
304 and *hemH*) and siroheme (*cysG*) synthesis, degradation (a heme oxygenase) and export (ABC-type
305 heme exporter, *ccmABCD*), as well as hemerythrin-like metal binding proteins were encoded.
306 Hemerythrin has been implicated in binding of oxygen for delivery to oxygen-requiring enzymes,
307 for detoxification, or for oxygen sensing in motile, microaerobic prokaryotes (French *et al.*, 2007).
308 The presence of these oxygen-dependent enzymes, as well as a key oxidative stress defense

309 enzyme superoxide dismutase (SOD), support the idea that *Chr. okenii* may be facultatively
310 microaerobic. A complete set of genes for flagellar biosynthesis (*fliDEGHIJKLMNOPQRW*,
311 *flgABCDEFGHIK*, *flhAB*) and flagellar motor proteins (*motAB*) confer motility to this bacterium.

312 Several other genes revealed interesting metabolic capacities of *Chr. okenii*. A cytosolic
313 bidirectional [NiFe] type 3d hydrogenase and a nitrogenase were encoded in the MAG (Fig. 4),
314 implicating the potential for involvement of *Chr. okenii* in nitrogen fixation and hydrogen
315 oxidation which has previously been overlooked. Additionally, the *Chr. okenii* MAG encoded a
316 glycogen synthase and a glycogen debranching enzyme, as well as the full genomic repertoire
317 necessary for polyhydroxyalkanoate (PHA) biosynthesis. This is consistent with the detection of
318 glycogen in our biogeochemical profiles of the chemocline. Finally, it is possible that novel
319 terminal oxidases are among the hypothetical genes that could not be assigned any known
320 function.

321 **CONCLUSIONS**

322 It is intriguing that oxygen should play a major role in sulfide oxidation in the ostensibly anoxic
323 chemocline of Lake Cadagno, especially by purple sulfur bacteria generally thought to lead an
324 anaerobic lifestyle. To explain the coupling of oxygen and sulfide consumption in the oxygen- and
325 sulfide-free chemocline of Lake Cadagno, we sketched a diagram of the transport processes likely
326 driving biological activity in the chemocline (Fig. 5). As described in Sommer *et al.*, (2017), active
327 convection of the chemocline can be driven by the formation of sinking bacterial plumes.
328 Combined with turbulence induced by the breaking of internal waves at sides of the lake basin,
329 these convective currents may entrain sulfide and oxygen at the boundaries of the chemocline
330 and fuel populations of sulfide-oxidizing *Chr. okenii* there.

331 Sulfur-oxidizing bacteria have previously been reported to bridge distances between pools of
332 electron donors and acceptors by intracellularly storing and transporting S^0 and NO_3^- between
333 redox zones (Fossing *et al.*, 1995; Jørgensen and Gallardo, 1999) and even by transferring
334 electrons along nanowires (Pfeffer *et al.*, 2012), but the sulfide oxidation processes in Lake
335 Cadagno represent a new mechanism of electron acceptor/donor coupling across large distances.
336 After entrainment into the chemocline, dissolved oxygen and sulfide are consumed so rapidly that
337 they remain below detection limits. Our metagenomic evidence shows that *Chr. okenii* possesses
338 several high-affinity oxidases which may enable it to respire oxygen at such low, nanomolar
339 concentrations. The physical and biological processes described here may therefore provide clues
340 to sulfide oxidation in other anoxic environments such as the Black Sea where the mechanism of
341 sulfide removal is not completely understood. Clearly, the biochemical limits to oxygen utilization
342 are far below current definitions of *anoxia* and demonstrate that aerobic respiration is possible
343 in so-called “anoxic” lacustrine (Milucka *et al.*, 2015) and marine (Garcia-Robledo *et al.*, 2017)
344 waters.

345 Overall, we show that in contrast to observations from laboratory cultures, *Chr. okenii* appear to
346 have a very different metabolism in the environment where high fluxes of nutrients rather than
347 absolute nutrient concentrations fuel microbial activity. The unexpected insights into the
348 ecophysiology of the purple sulfur bacteria obtained here demonstrate the importance of
349 studying these versatile bacteria *in situ* using culture-independent methods to understand their
350 environmental function.

351 **EXPERIMENTAL PROCEDURES**

352 **Sampling**

353 The meromictic Lake Cadagno is situated in the Piora Valley in the Swiss Alps at an altitude of
354 1921 m. Data presented here were collected during field campaigns in September 2013, August
355 2014, June 2015 and August 2015. In 2013 and 2014 *in situ* measurements were performed with
356 a profiling ion analyzer (PIA; see Kirf *et al.*, 2014 for description) lowered from a platform
357 anchored at the deepest part of the lake (20.7 m). Conductivity, turbidity, depth (pressure),
358 temperature and pH were measured with a multi-parameter probe (XRX 620, RBR). Dissolved
359 oxygen was recorded online with a type PSt1 normal (detection limit 125 nM) micro-optode and
360 a type TOS7 trace (reliable detection limit 50-100 nM) micro-optode (PreSens). The oxygen
361 sensors were calibrated by parallel Winkler titrations. Water samples for chemical analyses and
362 cell counts were collected with a rosette syringe sampler equipped with twelve 60-ml syringes
363 triggered online at selected depths. Due to a technical failure of the PIA, the 6 AM profile in August
364 2014 and all subsequent profiles in 2015 were measured with a SBE 19 plus V2 CTD probe (Sea-
365 Bird Electronics, WA, USA) equipped with sensors for pressure, temperature and conductivity,
366 and with additional sensors for turbidity (WET Labs Eco), oxygen (SBE 43), pH (18-I) and two
367 fluorescence wavelengths (WET Labs ECO-AFL, FL, USA). The detection limit of the SBE 43 oxygen
368 probe was about 1 $\mu\text{mol/l}$. In parallel with *in situ* measurements, water for chemical analyses was
369 pumped to the surface through Neoprene tubing attached to the CTD and filled into 60-ml
370 syringes (rinsed 2 X with *in situ* water) on board. Two parallel metal plates of diameter ~ 15 cm
371 attached to the submersed end of the tubing served to channel water horizontally, resulting in
372 more discrete vertical profiling.

373 Water samples in syringes were aliquoted on board immediately after collection. Samples for
374 sulfate analyses were filtered (0.22 μm pore size) directly into sterile Eppendorf vials. Sulfide

375 samples were fixed with Zn-acetate to a final concentration of 0.1 % (w/v). Biomass was
376 concentrated onto glass fiber filters (0.7 μm pore size) and stored at -20°C for analyses of
377 intracellularly stored elemental sulfur and organic carbon compounds. Filtrate (0.22 μm pore size)
378 was also collected and frozen at -20°C for metabolome analysis of dissolved compounds. Samples
379 for fluorescence *in situ* hybridization were immediately fixed with 2% (v/v) formaldehyde.
380 Samples for DNA analysis were collected from the chemocline in August 2014 by concentrating
381 microbial cells on polycarbonate filters (0.22 μm pore size) on site and freezing at -20°C until
382 further processing.

383 Additional water for cultivation and motility experiments was pumped directly from the
384 chemocline into 1-L Duran bottles and sealed with butyl rubber stoppers without a headspace to
385 maintain anoxic conditions.

386 **Chemical Analyses**

387 Sulfide was measured using the colorimetric method of Cline (1969). Sulfate was measured on a
388 761 Compact ion chromatograph (Metrohm, Filderstadt, Germany) equipped with a Metrosep A
389 SUPP 5 column. Intracellular sulfur on filters was extracted by sonication in methanol for 15 min
390 in an ice bath. Samples were analyzed on an Acquity H-Class UPLC system (Waters Corporation,
391 USA) with an Acquity UPLC BEH C18 column coupled to a photodiode array (PDA) detector using
392 UPLC-grade methanol as eluent. Data was acquired and processed using the Empower III
393 software.

394 Intracellular glycogen was analyzed following the procedures of the assay kit (MAK016 Sigma
395 Aldrich). Briefly, cells were extracted by scraping them from GFF filters and homogenizing in 200

396 μL extraction buffer and centrifuged two times to clear the supernatant. The supernatant was
397 analyzed fluorometrically after incubation with enzyme mix and fluorescent peroxidase substrate.
398 Intracellular PHA was analyzed using the protocol from Braunegg *et al.* (1978). Hydrolyzation of
399 the polymer and conversion to a methyl-ester of the monomeric hydroxyalkanoate fraction was
400 done in acidified alcohol solution (6% H_2SO_4 in methanol) and chloroform under heating (100°C ,
401 2h). After addition of water and phase separation the organic phase was analyzed with GC-MS
402 (Agilent 7890B GC connected to Agilent 5977A MSD) to detect the methylhydroxyalkanoates
403 using the following settings: Agilent 30 m DB-5-MS column, splitless injection of $1\ \mu\text{L}$, temperature
404 program was 50°C for 1min than heating $10^\circ\text{C}/\text{min}$ until 120°C followed by $45^\circ\text{C}/\text{min}$ until 320°C
405 and hold for 5 minutes. Benzoic acid was used as internal standard in each sample and
406 quantification was done with pure polyhydroxybutyrate standard (Sigma_Aldrich).

407 Sulfate reduction rates were measured by adding the radiotracer $^{35}\text{SO}_4^{2-}$ (5 MBq) to anoxic lake
408 water in 50-ml glass syringes and incubated in the dark. A solution of unlabeled Na_2S was added
409 to a final concentration of $\sim 50\ \mu\text{mol}\cdot\text{l}^{-1}$ as a background sulfide pool in case of sulfide re-oxidation.
410 At each sampling point, 10 ml of sample was dispensed into 5 ml of 20% (w/v) Zn-acetate.
411 Reduced sulfur species (e.g. sulfur and sulfide as ZnS) were separated out via the chromium
412 distillation method described in (Kallmeyer *et al.*, 2004) and the radioactivity per sample was
413 determined via scintillation counting (Packard 2500 TR).

414 **Confocal Raman spectroscopy**

415 In glove box under 90:10 $\text{N}_2\text{-CO}_2$ atmosphere, a drop of fresh sample from the chemocline was
416 mounted between two glass coverslips and sealed with electrical tape to prevent contact with

417 air. A polysulfide solution containing 5.06 g $\text{Na}_2\text{S} \cdot 9\text{H}_2\text{O}$ and 5.8 g elemental sulfur per 100 ml
418 H_2O , with a final pH of 9.5 and sulfide concentration of 210 mM was used as reference.
419 Measurements were conducted with an NTEGRA Spectra confocal spectrometer (NT-MDT,
420 Eindhoven, Netherlands) coupled to an inverted Olympus IX71 microscope. The excitation light
421 from a 532-nm solid-state laser was focused on the sample through an Olympus 100X (numerical
422 aperture [NA], 1.3) oil immersion objective. Raman scattered light was collected by an electron-
423 multiplying charge-coupled device (EMCCD) camera (Andor Technology, Belfast, Northern
424 Ireland) cooled to -70°C . Spectra were recorded between 0 and $4,500\text{ cm}^{-1}$ with a spectral
425 resolution of 0.2 cm^{-1} and analyzed with the software NT-MDT software Nova_Px 3.1.0.0.

426 **Flux Calculations**

427 Turbulent fluxes (J) of sulfide, sulfur, sulfate, and oxygen at the chemocline were calculated
428 assuming steady state by applying Fick's first law: $J = -D\partial C/\partial x$. For sulfide, sulfate, and oxygen we
429 used the turbulent diffusion coefficient (D) of $1.6 \times 10^{-6}\text{ m}^2\text{ s}^{-1}$ from (Wüest, 1994) corresponding
430 to turbulence at the Lake Cadagno chemocline boundaries. For sulfur gradients within the well-
431 mixed chemocline the coefficient $D = 1.5 \times 10^{-5}\text{ m}^2\text{ s}^{-1}$ (Wüest, 1994) was used. The change in
432 concentration (∂C) was computed for each species over the depths with the steepest gradients.
433 Oxygen and sulfide fluxes were determined for the regions immediately above and below the
434 chemocline, defined as the zone of constant conductivity.

435 **Microbial cultivation**

436 Anoxygenic phototrophic bacteria from the Lake Cadagno chemocline were cultivated in agar-
437 stabilized, sulfide gradient medium in anoxic test tubes. Solid agar (1.5% w/v agar) and semi-solid
438 agar (0.25% w/v agar) were prepared separately by autoclaving triple-washed agarose and sterile-

439 filtered water from the Lake Cadagno chemocline, and degassing for 1 h with mixture of 80% N₂
440 and 20% CO₂ during cooling to ~50°C. The solid agar was amended with a sterile Na₂S solution to
441 a final concentration of ~4mM before pouring into degassed test tubes to form a ~2 cm bottom
442 layer and allowed to set. The semisolid agar was amended with vitamins and trace elements as
443 described for cultivation of purple sulfur bacteria (Eichler and Pfennig, 1988) before pouring a ~7
444 cm top layer, and immediately capped with a butyl rubber stopper. After cooling to ~30°C, 1 ml
445 of fresh Cadagno chemocline water was used to inoculate the top agar via a degassed syringe.
446 Tubes were inverted once to mix and allowed to set. Agar cultures were incubated under low, 24-
447 h light conditions at 15°C to favor the development of anoxygenic phototrophs.

448 **Microsensor measurements**

449 Gradients of pH and H₂S in agar cultures were measured using microelectrodes built in-house as
450 described previously (Jeroschewski *et al.*, 1996; de Beer *et al.*, 1997). Immediately before use, the
451 pH sensor was calibrated in standard buffers and the H₂S sensor was calibrated in a dilution series
452 of an acidified Na₂S solution. Electrodes were mounted on a micromanipulator connected to a
453 computer and profiles were measured in 250 μm intervals from the agar surface to the base of
454 the sulfide plug. Agar tubes were uncapped for the insertion of microsensors, and the headspace
455 was flushed with N₂ gas before recapping immediately after each measurement. Total sulfide
456 concentrations were calculated from pH and H₂S gradients as described in Schwedt *et al.*, (2012).

457 **Motility analysis**

458 Water samples containing *Chr. okenii* cells were collected under anoxic conditions from the
459 chemocline during the night, protected from artificial light with aluminum foil, and analyzed

460 immediately on site. Motile cells were transferred via a degassed glass syringe to a sealed
461 rectangular millimetric chamber (dimensions 20 mm × 10 mm × 2 mm) prepared using glass slides
462 separated by a 2-mm thick spacer, which provided an anoxic environment during motility
463 characterization. Experiments were conducted in a dark room, and imaging was performed using
464 the dark field microscopy mode at 25 fps, with the lowest intensity illumination. No transient
465 response was observed right at the start of the imaging, and the swimming velocity remained
466 steady throughout the duration of the measurements. This is in contrast to swimming behavior
467 at higher light intensities where the swimming cells exhibited a positive phototactic response
468 (Sommer *et al.*, 2017). We could therefore rule out a light-induced effect on motility at the
469 minimum illumination level used for our measurements. Videos of swimming cells were acquired
470 and subsequently analyzed using the ImageJ Particle Tracker routine to obtain the coordinates of
471 the cells (geometric centers) at each time interval. These were used to calculate the swimming
472 speeds and extract the trajectories of individual cells.

473 **DNA extraction, sequencing, and analysis**

474 Environmental DNA was extracted from polycarbonate filters with the Ultra Clean MoBio
475 PowerSoil DNA kit (MoBio Laboratories, Carlsbad, USA) according to the manufacturer's protocol
476 with the following modification: the bead beating step was reduced to 30 sec followed by
477 incubation on ice for 30 sec, repeated 4x. The DNA was gel-purified using SYBR Green I Nucleic
478 Acid Gel Stain (Invitrogen) and the QIAquick Gel Extraction Kit (Qiagen) according to the
479 accompanying protocols. DNA concentration was determined fluorometrically at 260 nm, using
480 the Qubit 2.0 Fluorometer and the Qubit dsDNA HS Assay KIT (Invitrogen) and sent to the Max
481 Planck-Genome Centre (Cologne, Germany) for sequencing. The metagenome was sequenced

482 (100 bp paired end reads) by Illumina HiSeq (Illumina Inc., USA) sequencing following a TruSeq
483 library preparation. Metagenomic reads were adapter- and quality-trimmed (phred score 15,
484 bbdduk function of the BBMap package, <https://sourceforge.net/projects/bbmap/>) and paired-
485 end reads were *de novo* assembled with the uneven depth assembler IDBA-UD (Peng *et al.*, 2012).
486 The metagenome assembly was binned based on tetranucleotide frequencies, differential
487 coverage, taxonomic classification, and conserved single-copy gene profiles with the Metawatt
488 binning software (version 3.5.2; Strous *et al.*, 2012). The completeness and contamination of the
489 binned MAGs was evaluated with CheckM (Parks *et al.* 2014). The bulk metagenome and the MAG
490 identified as *Chr. okenii* were automatically annotated in IMG (Markowitz *et al.* 2011), and the *Chr.*
491 *okenii* MAG was manually screened for the presence of genes of interest to this study. Assembled
492 data is available in IMG, under the IMG genome IDs 3300010965 (bulk assembly) and 2700988602
493 (*Chr. okenii* MAG).

494 **ACKNOWLEDGEMENTS**

495 We are grateful to the 2014 and 2015 Cadagno Field Expedition Teams from EAWAG and MPI
496 Bremen for assistance in the field, and to the Alpine Biology Center Foundation (Switzerland) for
497 use of its research facilities. We would especially like to thank Dolma Michellod, Kirsten Oswald,
498 Daniela Tienken and Samuel Luedin for technical support. Funding was provided by the
499 International Max Planck Research School of Marine Microbiology, the Max Planck Society, and
500 the Deutsche Forschungsgemeinschaft (through the MARUM Center for Marine Environmental
501 Sciences). A.S. was supported by the Human Frontier Science Program (Cross Disciplinary
502 Fellowship, LT000993/2014-C).

503

504 **REFERENCES**

- 505 Berg, J.S., Schwedt, A., Kreutzmann, A.-C., Kuypers, M.M., and Milucka, J. (2014) Polysulfides as
506 Intermediates in the Oxidation of Sulfide to Sulfate by *Beggiatoa* spp. *Applied and Environmental*
507 *Microbiology* **80**: 629-636.
- 508 Braunegg, G., Sonnleitner, B. Y., and Lafferty, R. M. (1978). A rapid gas chromatographic method for the
509 determination of poly- β -hydroxybutyric acid in microbial biomass. *Applied Microbiology and*
510 *Biotechnology*, *6*(1), 29-37.
- 511 Cline, J.D. (1969) Spectrophotometric determination of hydrogen sulfide in natural waters. *Limnology and*
512 *Oceanography* **14**: 454-458.
- 513 Dahl, C., Engels, S., Pott-Sperling, A. S., Schulte, A., Sander, J., Lübbe, Y., ... and Brune, D. C. (2005). Novel
514 genes of the *dsr* gene cluster and evidence for close interaction of *Dsr* proteins during sulfur oxidation in
515 the phototrophic sulfur bacterium *Allochromatium vinosum*. *Journal of Bacteriology*, *187*(4), 1392-1404.
- 516 Dahl, T.W., Anbar, A.D., Gordon, G.W., Rosing, M.T., Frei, R., and Canfield, D.E. (2010) The behavior of
517 molybdenum and its isotopes across the chemocline and in the sediments of sulfidic Lake Cadagno,
518 Switzerland. *Geochimica et Cosmochimica Acta* **74**: 144-163.
- 519 De Beer, D. I. R. K., Schramm, A., Santegoeds, C. M., and Kuhl, M. (1997). A nitrite microsensor for profiling
520 environmental biofilms. *Applied and Environmental Microbiology*, *63*(3), 973-977.
- 521 De Witt, R., and Van Gemerden, H. (1990) Growth of the phototrophic purple sulfur bacterium
522 *Thiocapsaroseopersicina* under oxic/anoxic regimens in the light. *FEMS Microbiology Ecology* **6**: 69-76.
- 523 Del Don, Chr., Hanselmann, K.W., Peduzzi, R., and Bachofen, R. (1994) Biomass composition and methods
524 for the determination of metabolic reserve polymers in phototrophic sulfur bacteria. *Aquatic Sciences* **56**:
525 1-15.
- 526 Egli, K., Wiggli, M., Klug, J., and Bachofen, R. (1998) Spatial and temporal dynamics of the cell density in a
527 plume of phototrophic microorganisms in their natural environment. *Doc Ist Ital Idrobiol* **63**: 121-126.
- 528 Findlay, A.J., Bennett, A.J., Hanson, T.E., and Luther, G.W. (2015) Light-dependent sulfide oxidation in the
529 anoxic zone of the Chesapeake Bay can be explained by small populations of phototrophic bacteria.
530 *Applied and Environmental Microbiology* **81**: 7560-7569.
- 531 Forte, E., Borisov, V. B., Falabella, M., Colaço, H. G., Tinajero-Trejo, M., Poole, R. K., ... and Giuffrè, A.
532 (2016). The terminal oxidase cytochrome *bd* promotes sulfide-resistant bacterial respiration and growth.
533 *Scientific Reports*, *6*, 23788.
- 534 Fossing, H., Gallardo, V., Jorgensen, B., Hiittel, M., Nielsen, L., Schulz, H. *et al.*, (1995) Concentration and
535 transport of nitrate by the mat-forming sulphur bacterium *Thioploca*. *Nature* **374**: 20.
- 536 French, C. E., Bell, J. M., and Ward, F. B. (2007). Diversity and distribution of hemerythrin-like proteins in
537 prokaryotes. *FEMS Microbiology Letters*, *279*(2), 131-145.
- 538 Garcia-Robledo, E., Padilla, C. C., Aldunate, M., Stewart, F. J., Ulloa, O., Paulmier, A., ... and Revsbech, N.
539 P. (2017). Cryptic oxygen cycling in anoxic marine zones. *Proceedings of the National Academy of Sciences*,
540 201619844.

- 541 Halm, H., Musat, N., Lam, P., Langlois, R., Musat, F., Peduzzi, S. *et al.*, (2009) Co-occurrence of
542 denitrification and nitrogen fixation in a meromictic lake, Lake Cadagno (Switzerland). *Environmental*
543 *Microbiology* **11**: 1945-1958.
- 544 Imhoff, J. F., Süling, J., and Petri, R. (1998). Phylogenetic relationships among the Chromatiaceae, their
545 taxonomic reclassification and description of the new genera *Allochromatium*, *Halochromatium*,
546 *Isochromatium*, *Marichromatium*, *Thiococcus*, *Thiohalocapsa* and *Thermochromatium*. *International*
547 *Journal of Systematic and Evolutionary Microbiology*, **48**(4), 1129-1143.
- 548 Janz, G., Downey Jr, J., Roduner, E., Wasilczyk, G., Coutts, J., and Eluard, A. (1976) Raman studies of sulfur-
549 containing anions in inorganic polysulfides. Sodium polysulfides. *Inorganic Chemistry* **15**: 1759-1763.
- 550 Jeroschewski, P., Steuckart, C., and Kühl, M. (1996). An amperometric microsensor for the determination
551 of H₂S in aquatic environments. *Analytical Chemistry*, **68**(24), 4351-4357.
- 552 Jørgensen, B.B., Fossing, H., Wirsén, Chr.O., and Jannasch, H.W. (1991) Sulfide oxidation in the anoxic Black
553 Sea chemocline. *Deep Sea Research Part A, Oceanographic Research Papers* **38**: S1083-S1103.
- 554 Jørgensen, B.B., and Gallardo, V.A. (1999) Thioploca spp.: filamentous sulfur bacteria with nitrate vacuoles.
555 *FEMS Microbiology Ecology* **28**: 301-313.
- 556 Kallmeyer, J., Ferdelman, T.G., Weber, A., Fossing, H., and Jørgensen, B.B. (2004) A cold chromium
557 distillation procedure for radiolabeled sulfide applied to sulfate reduction measurements. *Limnology and*
558 *Oceanography Methods* **2**: 171-180.
- 559 Kampf, Chr., and Pfennig, N. (1980) Capacity of Chromatiaceae for chemotrophic growth. Specific
560 respiration rates of *Thiocystis violacea* and *Chromatium vinosum*. *Archives of Microbiology* **127**: 125-135.
- 561 Kirf, M.K., Dinkel, Chr., Schubert, Chr.J., and Wehrli, B. (2014) Submicromolar oxygen profiles at the oxic-
562 anoxic boundary of temperate lakes. *Aquatic Geochemistry* **20**: 39-57.
- 563 Markowitz, V.M., Chen, I.M.A., Palaniappan, K., Chu, K., Szeto, E., Grechkin, Y., Ratner, A., Jacob, B., Huang,
564 J., Williams, P. and Huntemann, M., (2011). IMG: the integrated microbial genomes database and
565 comparative analysis system. *Nucleic Acids Research*, **40**(D1), pp.D115-D122.
- 566 Mas, J., and Van Gemerden, H. (1995) Storage products in purple and green sulfur bacteria. In *Anoxygenic*
567 *Photosynthetic Bacteria*: Springer, pp. 973-990.
- 568 Milucka, J., Kirf, M., Lu, L., Krupke, A., Lam, P., Littmann, S. *et al.*, (2015) Methane oxidation coupled to
569 oxygenic photosynthesis in anoxic waters. *The ISME Journal*.
- 570 Musat, N., Halm, H., Winterholler, B., Hoppe, P., Peduzzi, S., Hillion, F. *et al.*, (2008) A single-cell view on
571 the ecophysiology of anaerobic phototrophic bacteria. *Proceedings of the National Academy of Sciences*
572 **105**: 17861-17866.
- 573 Overmann, J. (1997) Mahoney Lake: a case study of the ecological significance of phototrophic sulfur
574 bacteria. In *Advances in Microbial Ecology*: Springer, pp. 251-288.
- 575 Parks DH, Imelfort M, Skennerton CT, Hugenholtz P, Tyson GW. 2014. Assessing the quality of microbial
576 genomes recovered from isolates, single cells, and metagenomes. *Genome Research*, **25**: 1043-1055

- 577 Peng, Y., Leung, H.Chr., Yiu, S.-M., and Chin, F.Y. (2012) IDBA-UD: a de novo assembler for single-cell and
578 metagenomic sequencing data with highly uneven depth. *Bioinformatics* **28**: 1420-1428.
- 579 Pfeffer, Chr., Larsen, S., Song, J., Dong, M., Besenbacher, F., Meyer, R.L. *et al.*, (2012) Filamentous bacteria
580 transport electrons over centimetre distances. *Nature* **491**: 218-221.
- 581 Pfennig, N. (1975). The phototrophic bacteria and their role in the sulfur cycle. *Plant and Soil*, *43*(1), 1-16.
- 582 Pfennig, N., Höfling, K.-H., and Kusmierz, H. (1968) *Chromatium okenii* (Thiorhodaceae)-Biokonvektion,
583 *aero-und phototaktisches Verhalten*: IWF.
- 584 Polerecky, L., Adam, B., Milucka, J., Musat, N., Vagner, T., and Kuypers, M.M. (2012) Look@ NanoSIMS—a
585 tool for the analysis of nanoSIMS data in environmental microbiology. *Environmental Microbiology* **14**:
586 1009-1023.
- 587 Posth, N. R., Bristow, L. A., Cox, R. P., Habicht, K. S., Danza, F., Tonolla, M., ... and Canfield, D. E. (2017).
588 Carbon isotope fractionation by anoxygenic phototrophic bacteria in euxinic Lake Cadagno. *Geobiology*.
- 589 Prange, A., Arzberger, I., Engemann, Chr., Modrow, H., Schumann, O., Trüper, H.G. *et al.*, (1999). *In situ*
590 analysis of sulfur in the sulfur globules of phototrophic sulfur bacteria by X-ray absorption near edge
591 spectroscopy. *Biochimica et Biophysica Acta (BBA)-General Subjects* **1428**: 446-454.
- 592 Schwedt, A., Kreutzmann, A. C., Polerecky, L., and Schulz-Vogt, H. N. (2012). Sulfur respiration in a
593 marine chemolithoautotrophic Beggiatoa strain. *Frontiers in Microbiology*, *2*, 276.
- 594 Socrates, G. (2004). *Infrared and Raman Characteristic Group frequencies: Tables and Charts*: John Wiley
595 and Sons.
- 596 Sommer, T., Danza, F., Berg, J., Sengupta, A., Constantinescu, G., Tokyay, T., Bürgmann, H., Dressler, Y.,
597 Sepúlveda Steiner, O., Schubert, C.J. and Tonolla, M. (2017). Bacteria-induced mixing in natural waters.
598 *Geophysical Research Letters*.
- 599 Storelli, N., Peduzzi, S., Saad, M.M., Frigaard, N.-U., Perret, X., and Tonolla, M. (2013) CO₂ assimilation in
600 the chemocline of Lake Cadagno is dominated by a few types of phototrophic purple sulfur bacteria. *FEMS*
601 *Microbiology Ecology* **84**: 421-432.
- 602 Strous, M., Kraft, B., Bisdorf, R., and Tegetmeyer, H. (2012) The binning of metagenomic contigs for
603 microbial physiology of mixed cultures. *Frontiers in Microbiology* **3**: 410.
- 604 Tonolla, M., Demarta, A., Peduzzi, R., and Hahn, D. (1999) *In situ* analysis of phototrophic sulfur bacteria
605 in the chemocline of meromictic Lake Cadagno (Switzerland). *Applied and Environmental Microbiology* **65**:
606 1325-1330.
- 607 Tonolla, M., Peduzzi, S., Demarta, A., Peduzzi, R., and Dittmar, H. A. H. N. (2004). Phototropic sulfur and
608 sulfate-reducing bacteria in the chemocline of meromictic Lake Cadagno, Switzerland. *Journal of*
609 *Limnology*, *63*(2), 161-170.
- 610 Tonolla, M., Peduzzi, R., and Hahn, D. (2005) Long-term population dynamics of phototrophic sulfur
611 bacteria in the chemocline of Lake Cadagno, Switzerland. *Applied and Environmental Microbiology* **71**:
612 3544-3550.

- 613 Vaituzis, Z., and Doetsch, R. (1969) Motility tracks: technique for quantitative study of bacterial movement.
614 *Applied Microbiology* **17**: 584-588.
- 615 Van Gernerden, H. (1968) On the ATP generation by Chromatium in darkness. *Archiv für Mikrobiologie* **64**:
616 118-124.
- 617 Wüest, A. (1994) Interactions in lakes: Biology as source of dominant physical forces. *Limnologica Jena* **24**:
618 93-104.
- 619

Fig 1: (a) Combined oxygen (top) and sulfide (bottom) profiles of the Lake Cadagno water column revealing the persistence of an oxygen- and sulfide- free zone over a period of 48 hours, with contour lines indicating sulfide concentrations. The bold contour lines delimiting the region with $> 5 \mu\text{M}$ sulfide were used to define the chemocline in parallel profiles of *Chr. okenii* cell counts (b), particulate S^0 (c), and sulfate (d). Black dots represent sampling points for all parameters except O_2 which was measured with a microsensor mounted on a CTD probe. Shaded boxes represent dark periods between sunset at $\sim 20:50$ and sunrise at $\sim 6:10$. Time plots were interpolated from original profiles measured in August 2015 and are provided in Fig S1.

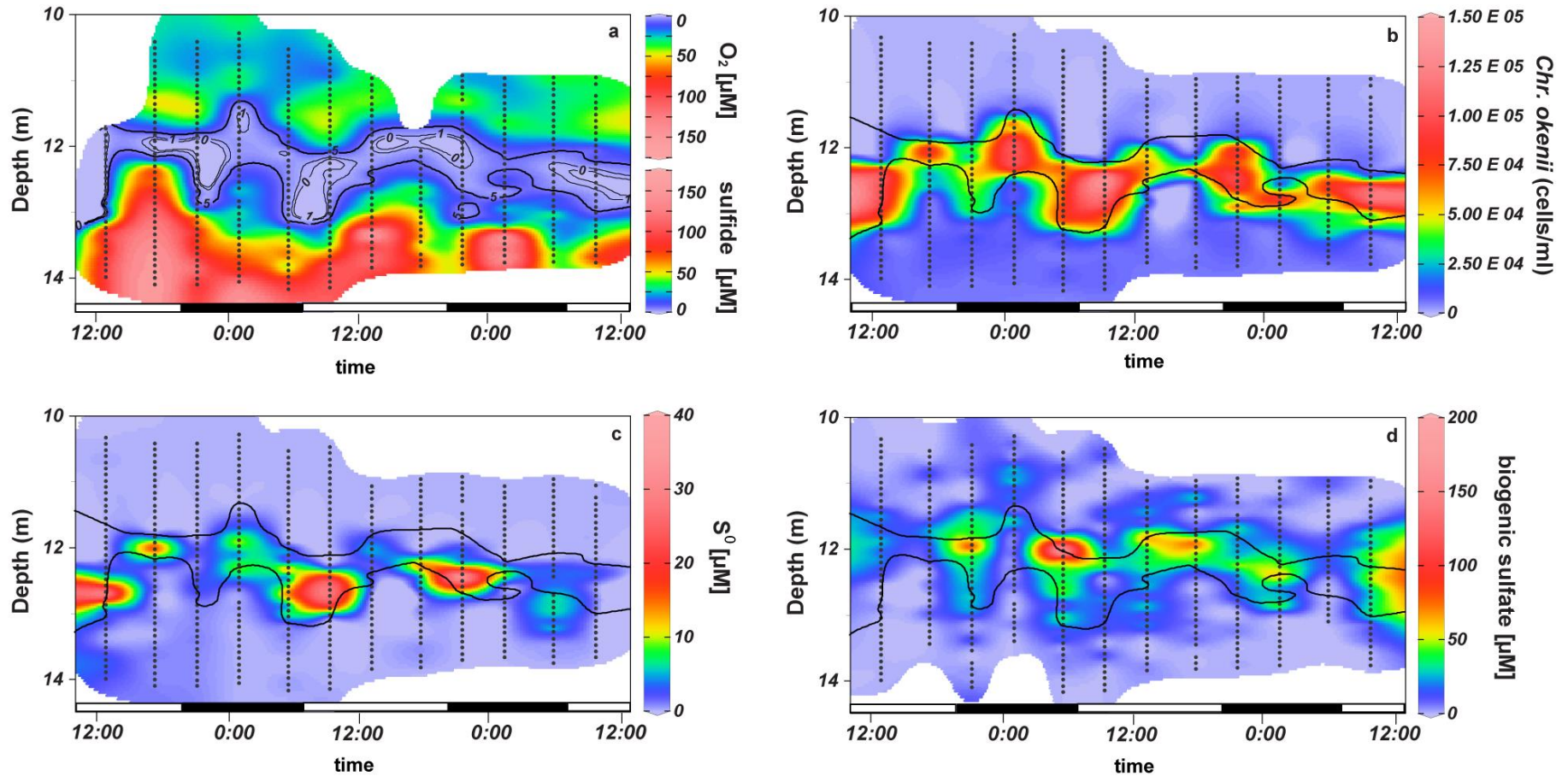


Figure 2: A day (13:00) and a night (1:30) profile through the chemocline illustrating glycogen and S^0 concentrations in relation to *Chr. okenii* cell numbers, oxygen, and sulfide gradients in the chemocline. Profiles were measured in August 2015. PHA was below detection limits and no oxygen data is available for the day profile.

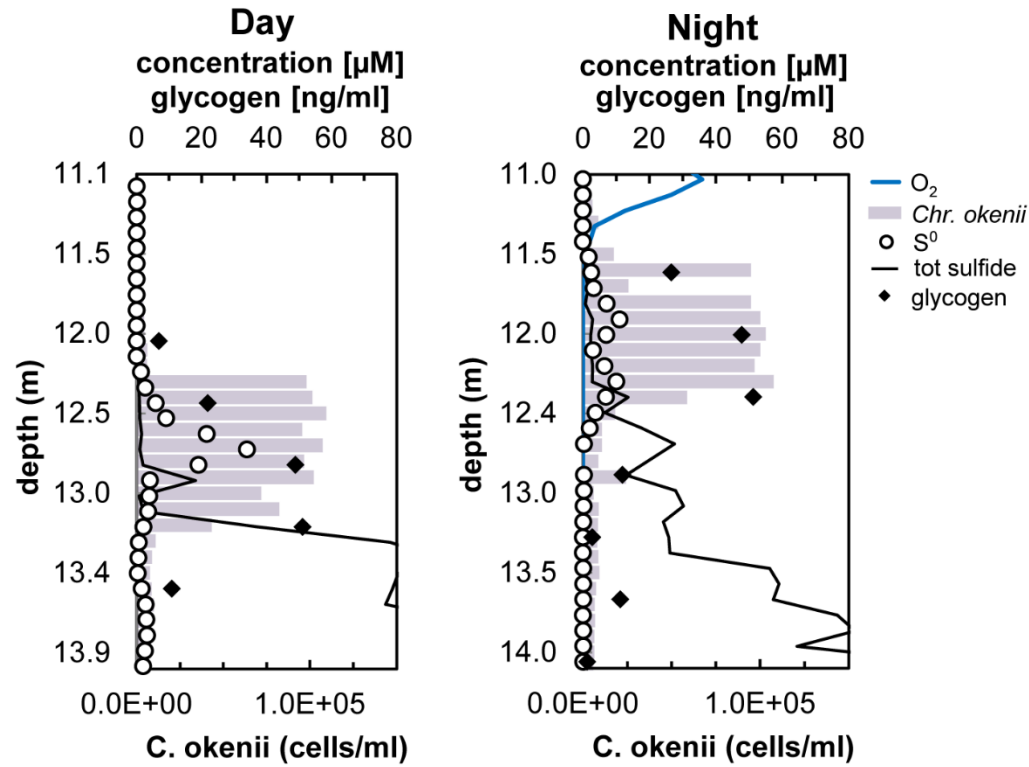


Figure 3: Sulfide and oxygen fluxes in the Lake Cadagno chemocline were calculated from profiles measured 4-h intervals over 2 day-night cycles. (a) The consumed sulfide flux (solid line) was calculated by subtracting the residual sulfide flux (dashed line) from the total sulfide flux into the mixed layer. (b) The downwards oxygen flux into the chemocline was used to estimate (c) the maximum % of sulfide aerobically respired, assuming the complete oxidation of sulfide to sulfate. Shaded regions represent dark periods.

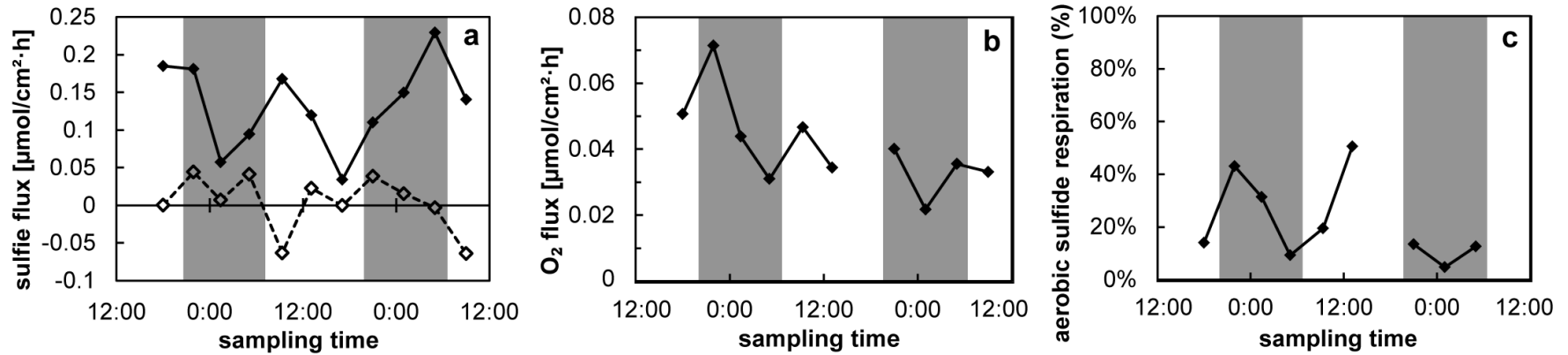


Figure 4: *Chr. okenii* cell illustration, showing the metabolic potential inferred from the metagenome-assembled genome with a particular focus on the genetic machinery implicated in photosynthesis, sulfur oxidation, aerobic metabolism, motility, glycogen and PHA storage, nitrogen fixation and transmembrane transport. The respiratory chain enzyme complexes are labeled with Roman numerals.

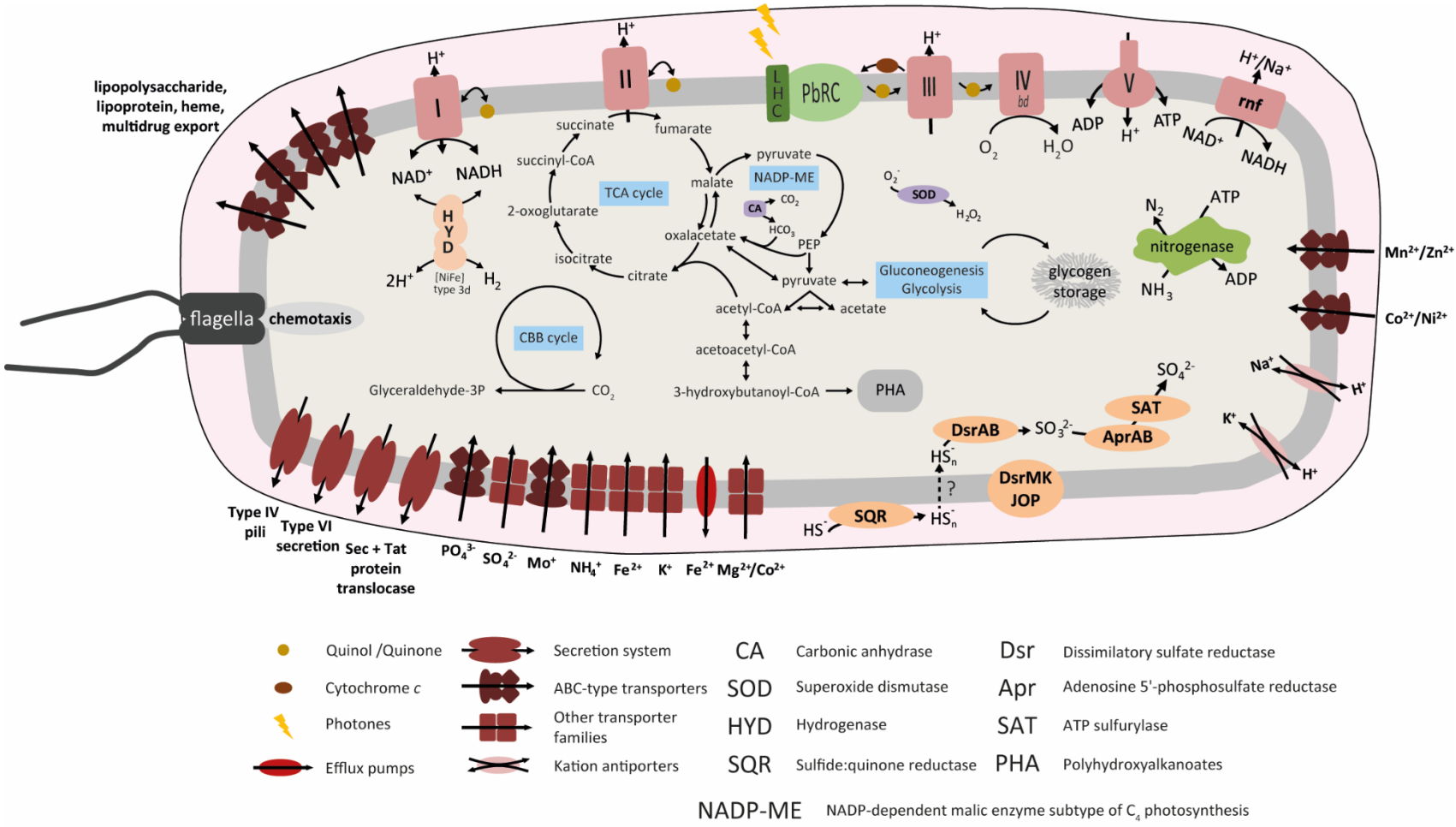


Figure 5: Schematic of phototrophic and aerobic sulfide oxidation processes in the Lake Cadagno chemocline. Convection in the chemocline may be driven by a combination of turbulence and sinking bacterial plumes, represented by the large number of descending *Chr. okenii* cells on the left. As a result, oxygen and sulfide are entrained into the chemocline and immediately consumed by purple sulfur bacteria, keeping concentrations of these compounds below detection limits. *Chr. okenii* cells, depicted with internal sulfur globules (yellow dots), are pulled in the direction of their flagellar bundle.

